Journal of
Aerospace Engineering & Technology

ISSN: 2231-038X (Online)
ISSN: 2348-7887 (Print)
Volume 15, Issue 3, 2025
September–December
DOI (Journal): 10.37591/JoAET

https://journals.stmjournals.com/joaet

Research JoAET

# Robust Design of Subsonic Airfoil by Multi-Objective Six Sigma Approach

Cha Chong Song, Ryu Tong Hwi, Kim Yong, Han Yong Gil*, Ho Myong Su, Kim Un Il

**_Abstract_**

*It is well known that aerodynamic performance of a UAV is very sensitive to the wing shape and flight conditions, and inevitable uncertainties such as wing manufacturing errors and wind variations may lead to drastic deterioration in its aerodynamic performance. In the UAV wing design, therefore, it is required not to use the conventional design optimization approach considering only optimality of performance at the design point, but to use the robust design optimization approach considering both optimality and robustness of performance against any uncertainties. The study describes a Multi-Objective Six Sigma Design of the subsonic airfoil with the purpose function of both the expected value and the dispersion of the lift-to-drag ratio of the airfoil with respect to the Mach number and the attack angle. First, it shows that the optimal control points of the cubic B-spline are obtained by means of the Integer Quadratic Programming for the initial airfoil. Finally, the robust design of airfoil was carried out with the aid of Isight 2017, regarding the obtained control points as the design variables and under consideration of the uncertainty of Mach number and attack angle. Here, the Multi-Objective Six Sigma Design of the airfoil was done in combination of six sigma analysis based on Monte-Carlo method with Multi-Objective Particle Swarm method to improve the optimization and robustness of the lift-to-drag ratio. A new optimization approach for robust design, Multi-Objective Six Sigma Design, has been developed and applied to robust aerodynamic airfoil design for subsonic UAV. The present robust aerodynamic airfoil design optimization using this approach successfully showed robustness improvement in aerodynamic performance. The obtained result indicated that an airfoil with a smaller maximum camber improves robustness of lift to drag ratio against the variation of flight Mach number and attack angle.*

**Keywords:** Airfoil, robust design, multi-objective six sigma analysis, lift to drag ratio, spline approximation

## INTRODUCTION

In real-world engineering designs, performance of a design may be very different from its expected value due to errors and uncertainties in design process, manufacturing process, and/or operating condition.

*Author for Correspondence
Han Yong Gil
E-mail: YG.HAN@star-co.net.kp

Professor, Department of Mechanical Science and Technology, Kim Chaek University of Technology, Pyongyang, Democratic People's Republic of Korea

Receiving Date: June 30, 2025
Accepted Date: September 18, 2025
Published Date: September 25, 2025

**Citation:** Cha Chong Song, Ryu Tong Hwi, Kim Yong, Han Yong Gil, Ho Myong Su and Kim Un Il. Robust Design of Subsonic Airfoil by Multi-Objective Six Sigma Approach. Journal of Aerospace Engineering & Technology. 2025; 15(3): 14–23p.

A typical example of such could be found in the airfoil design. It is well known that aerodynamic performance of airfoil is very sensitive to the airfoil shapes and flight conditions, and also the inevitable uncertainties like airfoil manufacturing errors, abrupt maneuver, payload, and wind variations may lead to drastic deterioration in aerodynamic performance.

In the airfoil design, therefore, it is required not to use the conventional design optimization approach in regard to optimal performance only, but to use the robust design optimum approach with regard to both of them for better performance against different uncertainties. Lots of robust optimum approaches have been projected, providing a reliable and useful information for airfoil design. Of them, six sigma design approach is sure to be one that just fits the most popular robust optimization for its simplicity and practicality [1–10]. Additionally, Table 1 represents the nomenclature of the used terminologies.

Here, the optimal control points for modeling the cubic B-spline parameters of the initial airfoil were firstly obtained by the integer quadratic programming.

And next, with the obtained control points taken as the design variables and in consideration of the uncertainty of Mach number and attack angle under the corresponding flight conditions, the airfoil robust design approach was projected to improve the optimization of robustness of the lift to drag ratio, by six sigma analysis based on Monte-Carlo Method combined with Multi-Objective Particle Swarm Method.

## THE PARAMETRIC MODELING OF AIRFOIL BY B-SPLINE

For the airfoil design, the initial airfoil parameters were modeled by using the cubic B-spline. Here, using the integer quadratic programming, we determined the optimal control points of the B-spline that satisfy the necessary airfoil shape correctness with only a few control points.

### B-Spline Approximation

It is not suitable to approximate the very coordinates of the airfoil in form of the spline function. Because the series of node must be non-decrement, but the airfoil is nearly the close curve shape, it is impossible to select the $x$ -coordinates into the series of spline nodes [4].

Thus, by introducing auxiliary parameter that can be non-decrement, and by separating two auxiliary parameter equations, the spline approximation is carried out respectively.

The coordinates of the airfoil, $P_j(x_j, y_j)$ $(j = 0, 1, \cdots, N)$ are given counter clockwise (Figure 1).

**Table 1.** Nomenclature.

| | |
|---|---|
| $Ma_\infty$ | free stream Mach number |
| $\alpha$ | attack angle |
| $Re$ | Reynolds number |
| $\mu_f$, $\sigma_f$ | mean and standard deviation |
| $K$ | $\sigma_f$ level |
| $c_l$ | lift coefficient |
| $c_d$ | total drag coefficient |
| $N_{crit}$ | transition criterion |

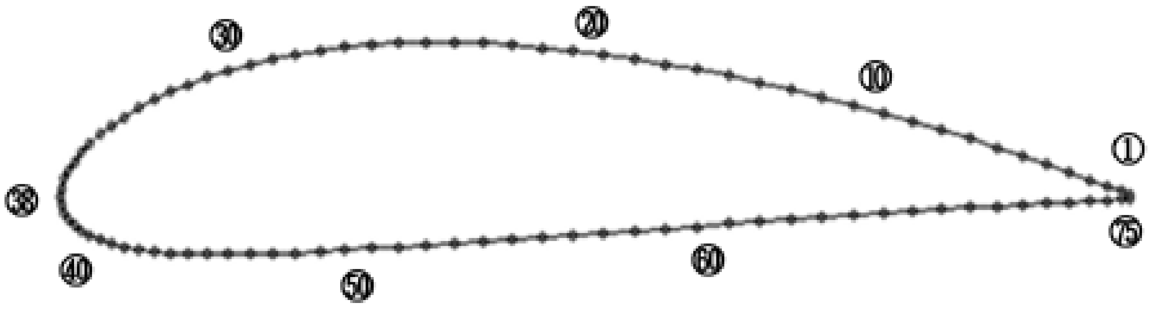


**Figure 1.** The node points of airfoil.

 

The curve length of the data points from $P_0$ to $P_i$ is chosen as the auxiliary variable.

$$t_j = \overline{P_0P_1} + \overline{P_1P_2} + \cdots + \overline{P_{j-i}P_j} = \sum_{i=1}^{j} \sqrt{(x_i - x_{i-1})^2 + (y_i - y_{i-1})^2} \quad (1)$$

As a result, the following new pairs of data can be obtained.

$$\left.\begin{matrix}(t_j, x_j)\\(t_j, y_j)\end{matrix}\right\}(j = 0, 1, \cdots, N)$$

Now, representing each curve of coordinates by using $k-1$th order spline with $n+1$ control points, $x(t)$ is as follows:

$$x(t) = \sum_{k=1}^{n+1} a_i B_{i,k}(t) \quad (2)$$

Where, $x(t)$ is the $x$ coordinate according to the curve length $t$of the airfoil and $a_i$ is the ordinate of $x(t)$ curve control points.

In Eq. (2), $B_{i,k}(t)$ is the B-spline base-function.

$$B_{i,k}(t) = \frac{(t-t_i)}{t_{i+k-1}-t_i} B_{i,k-1} + \frac{(t_{i+k}-t_i)}{t_{i+k}-t_{i+1}} B_{i+1,k-1}(t) \quad (3)$$

Where, $B_{i,1} = \begin{cases}1, & t_i \le t \le t_{i+1}\\ 0, & \text{etc.}\end{cases}$, $\boldsymbol{t} = [t_1, t_2, \cdots t_{n+k}]$ is the sample node vector and non-decrement series.

$$\begin{cases} x_1 = B_{1,k}(t_1)a_1 + B_{2,k}(t_1)a_2 + \cdots + B_{n+1,k}(t_1)a_{n+1}\\ x_2 = B_{1,k}(t_2)a_1 + B_{2,k}(t_2)a_2 + \cdots + B_{n+1,k}(t_2)a_{n+1}\\ \quad\cdots \qquad \cdots \qquad \cdots\\ x_j = B_{1,k}(t_j)a_1 + B_{2,k}(t_j)a_2 + \cdots + B_{n+1,k}(t_j)a_{n+1}\end{cases} \quad (4)$$

It is possible to calculate the control points of the B-spline curve that pass across the given sample points from Eq. (4).

$$[a] = [B]^{-1}[x] \quad (5)$$

Where, $[a] = [a_1, a_2, \cdots a_{n+1}]^T$, $[x] = [x_1, x_2, \cdots x_j]^T$, $[B] = \begin{bmatrix} B_{1,k}(t_1) \cdots B_{n+1,k}(t_1)\\ \cdots \quad \cdots \quad \cdots\\ B_{1,k}(t_j) \cdots B_{n+1,k}(t_j)\end{bmatrix}$ and $j$ should be satisfied with $n+1 \le j$ as the number of sample points.

Similarly, the spline approximation of $y(t)$ can be proceeded.

**Determination of the Optimal Control Points by the Integer Quadratic Programming**

In spline approximation of the airfoil, only when $n+1$ sample points are properly arranged, can the given shape correctness be satisfied with only a few control points and can the optimization efficiency be raised by decreasing the number of design variables.

Here, using Integer Quadratic Programming, the optimal control points of the cubic B-spline for the initial airfoil are determined, as shown in Figure 2 [5].

 

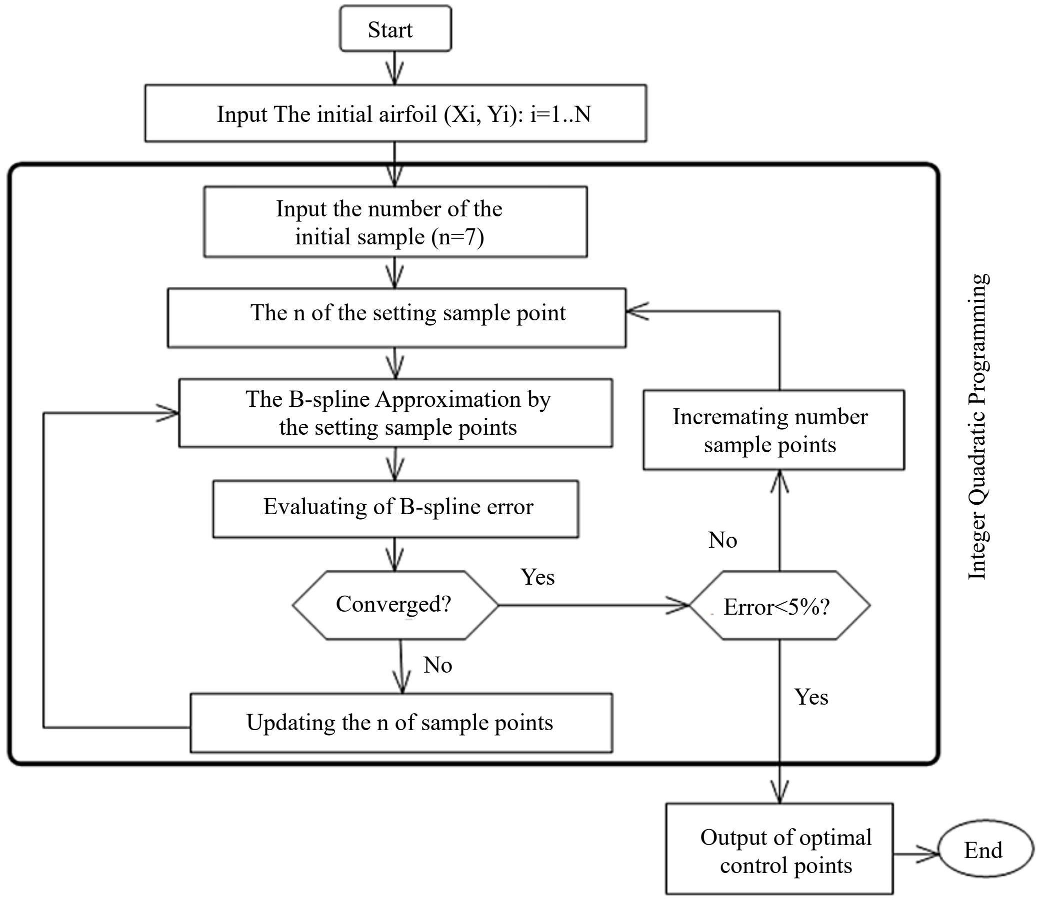


**Figure 2.** Determination of the optimal control points of the airfoil.

**Table 1.** The spline approximation error according to the numbers of control points.

| **Item** | **The number of control points** | | | |
|---|---|---|---|---|
| | 12 | 13 | 14 | 15 |
| Error (%) | 80 | 53 | 25 | 6.7 |
| Optimization method | Integer Quadratic Programming | | | |

The approximation errors of the cubic B-spline curve for the airfoil according to the number of control points are as follows;

As shown in Table 1, when at least 15 control points (if the trailing edge thickness is non-zero) are arranged rationally, the approximation error of the airfoil can be decreased by less than 7%.

The spline approximation curve of the airfoil for the obtained optimal control points is shown in Figure 3.

## THE AIRFOIL ROBUST DESIGN

The efficiency and capability of multi-objective six sigma design approach are investigated in order to provide the optimality and robustness of lift to drag ratio of the airfoil according to the variation of flight Mach number and attack angle.

The six sigma design ensures that the range of ±6σ (σ: standard deviation) around the design performance mean value μ can have the narrow dispersion within allowable range. The level of dispersion can be defined as "sigma level", where larger level σ means narrower distribution and it indicates better robustness for design [11–15].

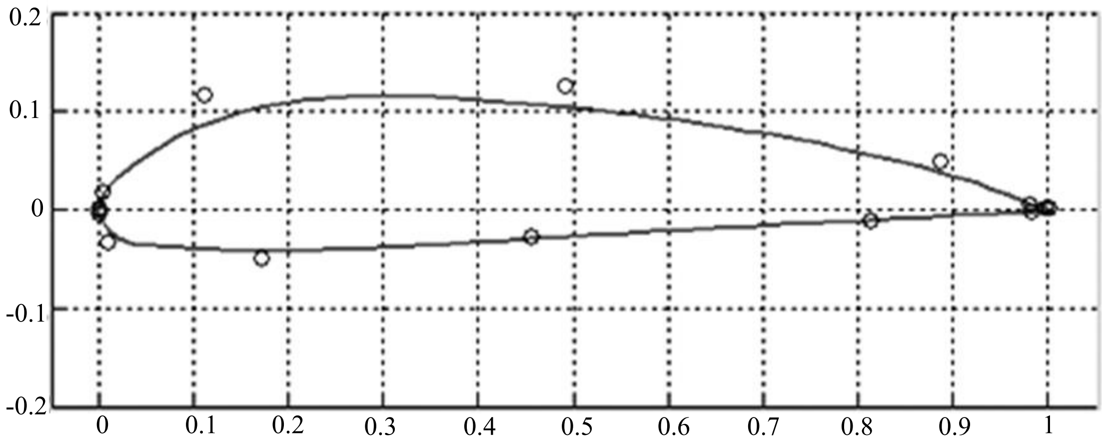


**Figure 3.** The parametric-modeling airfoil (NACA 4415).

In multi-objective six sigma design, if the control points of airfoil are set as the design variables, Mach number and attack angle as the factor of uncertainty, the mean value $\mu_f$ and standard deviation $\sigma_f$ for the lift to drag performance function $f(x, Ma_\infty, \alpha)$ as objective function, it is optimized as follows:

$$Minimize: -\mu_f \tag{6}$$

$$Minimize: {\sigma_f}^2 \tag{7}$$

$$x = (y_{c1}, y_{c2,} \dots, y_{ck-1}, , y_{ck})$$

$$Ly_{ci} \le y_{ci} \le Uy_{ci}$$

$$Ma_\infty \in [Ma_\infty^* - \varepsilon, Ma_\infty^* + \varepsilon]$$

$$\alpha \in [\alpha^* - \delta, \alpha^* + \delta]$$

$$\mu_f - n\sigma_f \ge LSL$$

Here, each element of the design variable vector$x$ is $y$-coordinate of the airfoil control points, $k$ is the number of control points, $Ly_{ci}$ and $Uy_{ci}$ are lower and upper $i$th variable limits, respectively, $n$ is the user-specified lower level of σ, $LSL$ is user-specified lower objective function limits. Here, upper objective function limits are not specified because a lift to drag ratio greater than the expected value $\mu_f$ is favorable in airfoil design.

Figure 4 illustrates the flowchart of robust airfoil design optimization using six sigma design approach.

"NACA 4415" airfoil is selected as the initial airfoil (Figure 3). Here, airfoil configuration is defined by the B-spline curves with two fixed points corresponding to trailing edges (if the trailing edge thickness is non-zero and there are two fixed control points or one fixed control) and 13 control points whose coordinates can be specified flexibly. The design variables are vertical (y) coordinates of the 13 control points.

This definition based on the B-spline curves has some advantages; the second-order derivative of coordinates along the B-spline curves is continuous and various airfoil configurations can be expressed.

In this study, the structural constraint on airfoil thickness is not considered because we discuss only the aerodynamic performance.

It is assumed that free stream Mach number $Ma_\infty$ is limited within range $[0.2,0.4]$ as normal distribution with mean value of 0.3 and standard deviation of 0.07, attack angle $\alpha$ disperses in a uniform distribution within range $[1, 7]$. Here, the value of 0.07 as the standard deviation of $Ma_\infty$ is equal to Mach variations considering the influence of wind velocity, balanced attack angle deviation, velocity measurement error, etc. The range $[1, 7]$ of attack angle is equal to the attack angle deviation due to the maneuver, change of payload, fuel consumption, wind, etc.

Also, Reynolds number is calculated based on flight altitude, Mach number and aerodynamic mean chord length $\bar{C} = 0.43$ ($Re = 2 \times 10^6 \sim 4 \times 10^6$).

For the design variable vector $x$, the values of objective function $\mu_f$ and $\sigma_f$ according to the uncertain flight parameters are estimated by the point estimation approach from the trial values.

$$\mu_f = \frac{1}{M}\sum_{i=1}^{M} L_i/D_i$$

$$\sigma_f = \frac{1}{M-1}\sum_{i=1}^{M}(L_i/D_i - \mu_f)^2 \tag{8}$$

Isight design flow diagram is shown as Figure 5.

For the initial airfoil, six sigma analysis result considering the uncertainty of the Mac number and attack angle is shown in Figure 6. In the optimization, the upper and lower limits of the design variable vector $x$ are given in Table 2.

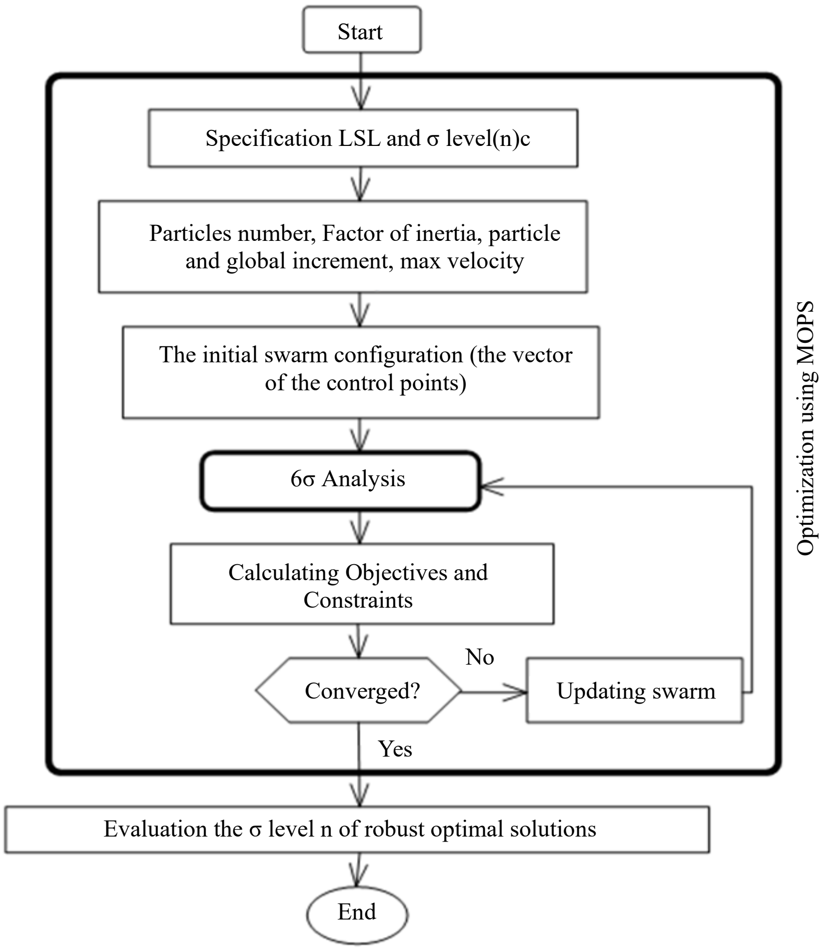


**Figure 4.** The flowchart of robust airfoil design optimization.

 

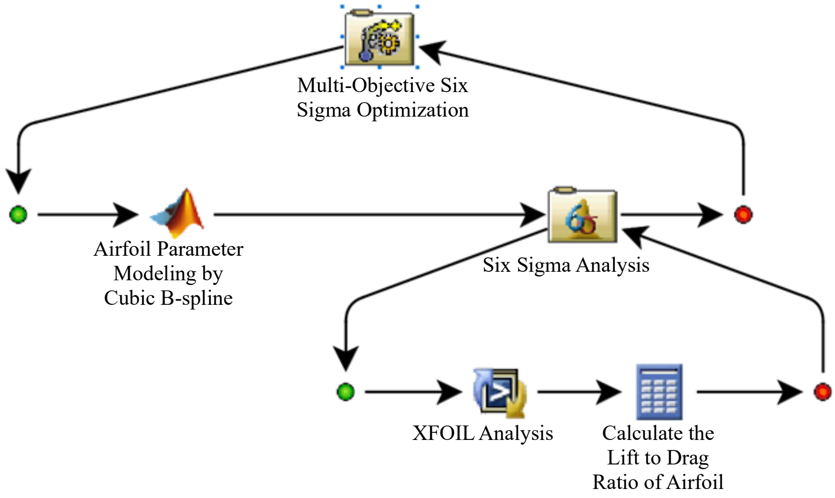


**Figure 5.** Isight design diagram.

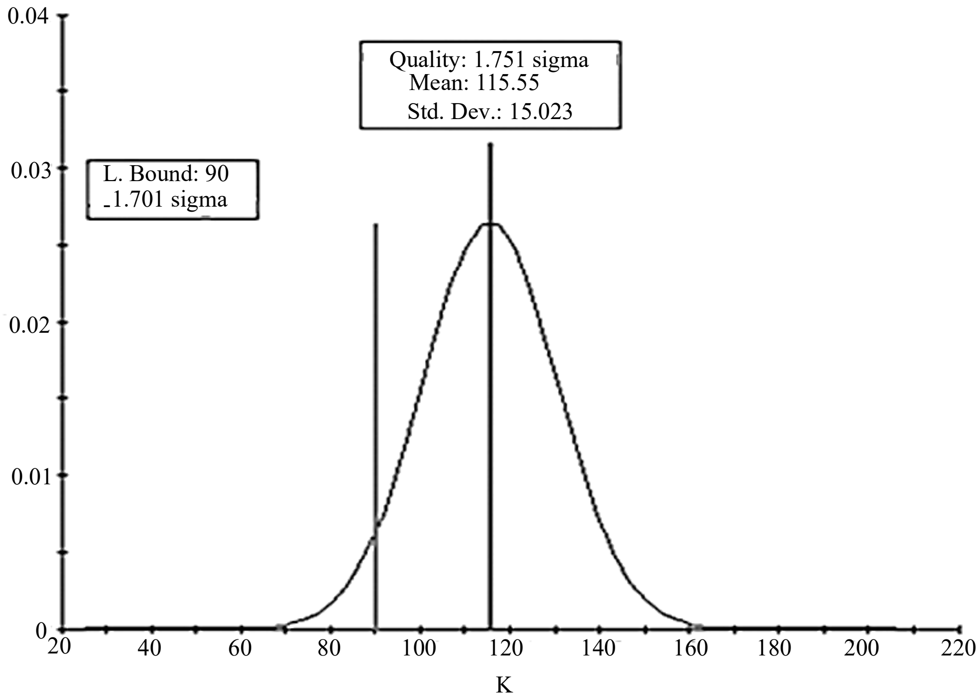


**Figure 6.** The lift to drag ratio distribution of the initial airfoil.

**Table 2.** Limits of the design variables.

| No. | Lower | Initial | Upper | No. | Lower | Initial | Upper |
|---|---|---|---|---|---|---|---|
| 1 | - | 0.00157 | - | 9 | –0.003 | –0.003449 | 0.0315 |
| 2 | 0.0021 | 0.00576 | 0.007 | 10 | –0.033 | –0.03236 | 0.0305 |
| 3 | 0.02 | 0.04977 | 0.06 | 11 | –0.05 | –0.04914 | 0.015 |
| 4 | 0.05 | 0.12583 | 0.14 | 12 | –0.028 | –0.02784 | 0.013 |
| 5 | 0.04 | 0.11642 | 0.13 | 13 | –0.011 | –0.01083 | 0.001 |
| 6 | 0.008 | 0.01866 | 0.053 | 14 | –0.0022 | –0.002193 | –0.0016 |
| 7 | 0.001 | 0.00251 | 0.048 | 15 | - | 0.00044 | - |
| 8 | –0.00046 | –0.00045 | 0.033 | | | | |

 

The parameters such as sigma lower level n and lower limit of the lift to drag ratio are predefined by the user: $LSL = 90$and $n = 6$. In each optimization process, the design variable vector $x$ is updated according to the optimal algorithm based on the Particle Swarm Method. Sigma level n satisfying with Eq. (7) is processed by sigma level assessment for the robust optimal solutions, as shown in Figure 7.

In the six sigma analysis, the numbers of trial for each uncertain flight parameter are 1000. And in the Multi-Objective Particle Swarm Method, the particles are 20, the inertia coefficient is 0.9, the coefficient of the particle increment is 0.9, the coefficient of global increment is 0.9 and the coefficient of the maximum velocity is 0.1.

The aerodynamic performance of airfoil is calculated using the 2D panel-boundary layer integrated analysis tool (XFOIL) that is widely utilized in the world.

The computational time taken for one calculation of aerodynamic performance (polar) of an airfoil using the XFOIL is about 1 sec, with processor of ASUS Dual Core and Win 7/64 bit OS. Also, the time taken for six sigma design of airfoil using Isight 2017 is about 10 h.

The optimal airfoil obtained by using six sigma design method is shown in Figure 7. The optimal airfoil has smaller relative thickness and the maximum camber than the initial airfoil. It shows that the airfoil with a smaller relative thickness and maximum camber improves the robustness of lift to drag ratio according to the uncertainty of the number of Mach and attack angle due to drop of pressure drag.

As shown in Figure 8 and Table 3, taking account for the uncertainty of Mach number and attack angle, the obtained airfoils are better than the initial: $\mu_f$, $\sigma_f$ and sigma level (lower) of the airfoil obtained by MOSS are 122.897, 5.283 and 6.226, while $\mu_f$, $\sigma_f$ and sigma level (lower) of the initial airfoil are 115.550, 15.023 and 1.701 respectively.

As shown in Figure 8, although it is considered only at $Ma_\infty = [0.2,0.4]$ and attack angle 1～7°, it can be seen that the optimal airfoil has better lift to drag characteristic than initial airfoil.

**Table 3.** The performance of the robust airfoil.

| Item | $\mu_f$ | $\sigma_f$ | *K lower* |
|---|---|---|---|
| Initial airfoil (NACA 4415) | 115.550 | 15.023 | 1.701 |
| Optimal airfoil | 122.897 | 5.283 | 6.226 |

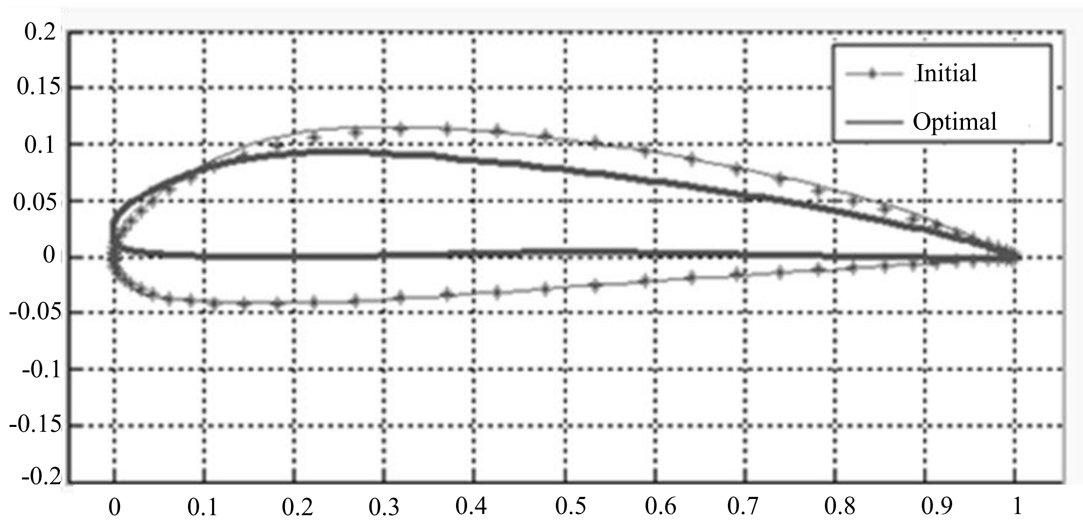


**Figure 7.** Robust airfoil obtained with MOSS.

 

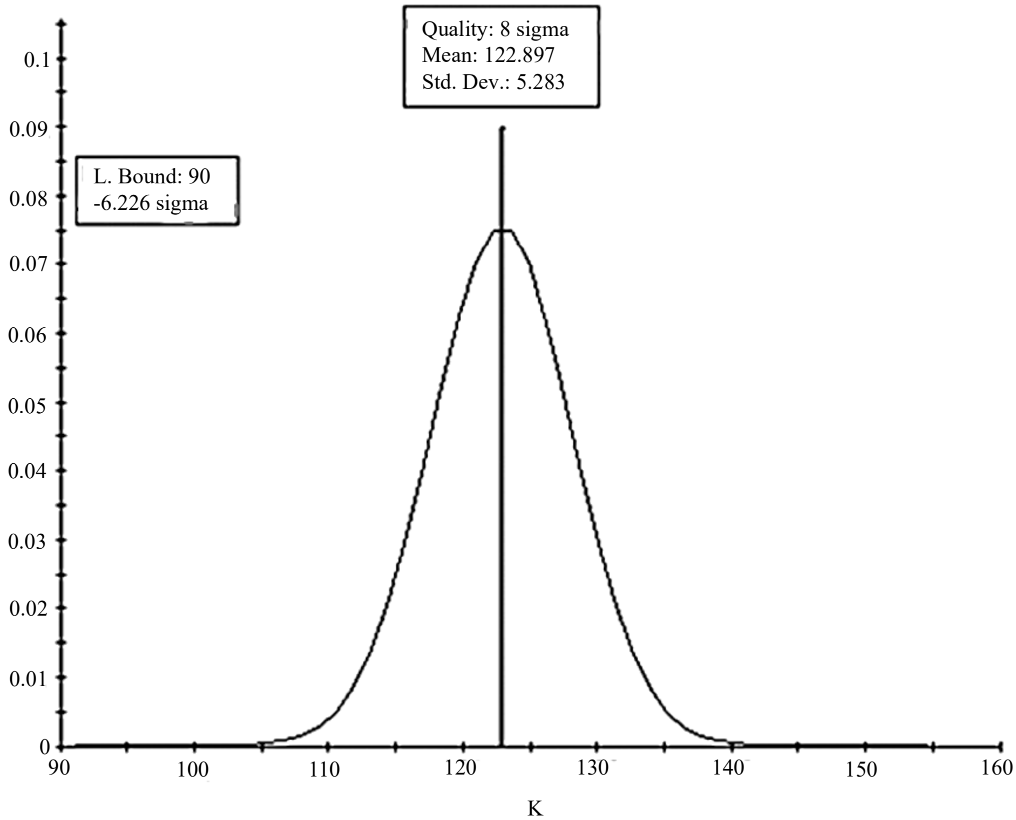


**Figure 8.** Distribution of the lift to drag ratio for the optimal airfoil.

## CONCLUSION

The study describes the Multi-Objective Six Sigma Design Approach and its determination of the Multi-Objective robust airfoil which satisfies both the optimum and robustness of lift to drag ratio in consideration of uncertainty that free stream Mach number $Ma_\infty$ is dispersed in a normal distribution with mean value of 0.3 and standard deviation of 0.07, and attack angle $\alpha$ is dispersed in a uniform distribution in the range $[1, 7]$.

Six sigma analysis and multi-objective six sigma design considering the uncertainties of flight parameters were conducted using Isight 2017, and the lift to drag characteristics were evaluated in XFOIL.

The comparison of the optimal airfoil with the initial one shows the improvements of characteristics of lift to drag ratio $\mu_f$ and $\sigma_f$ from 115.550 to 122.897 and from 15.023 to 5.283 each.

The optimal airfoil obtained by MOSS has a thinner profile and a lower maximum camber than the initial design, resulting in improved optimum performance and greater robustness in lift to drag ratio.

**Acknowledgements**

The authors would like to thank Prof. Dr. Kim Song Dong and Han Chol Min who gave valuable guidance in completing this study.

## REFERENCES

1. Elouardi S, El Maani R, Radi B. Probabilistic study of the aerodynamic around a 3D wing. Adv Theor Appl Mech. 2018; 11(1): 49–59.
2. Hollom J. Optimization of natural laminar flow aerofoils and wings for robustness to critical transition amplification factor. Thesis. Sheffield: The University of Sheffield; 2018; 13–162.

 

3. Zhang Y, Fang X, Chen H, Fu S, Duan Z, Zhang Y. Supercritical natural laminar flow airfoil optimization for regional aircraft wing design. Aerosp Sci Technol. 2017; 70: 568–577.
4. Tao J, Sun G, Si J, Wang Z. A robust design for a winglet based on NURBS-FFD method and PSO algorithm. Aerosp Sci Technol. 2015; 43: 152–164.
5. Engineous Software, Inc. Isight component guide. Version 2017.1. 2016; 134–193.
6. DeGennaro AM, Rowley CW, Martinelli L. Uncertainty quantification for airfoil icing using. J Aircraft. 2015; 52(5): 1404–1411.
7. Coder JG, Maughmer MD. Comparisons of theoretical methods for predicting airfoil aerodynamic characteristics. J Aircraft. 2014; 51(1): 183–191.
8. Li J, Gao Z, Huang J, Zhao K. Robust design of NLF airfoils. Chin J Aeronaut. 2013; 26(2): 309–318.
9. Ghadimi P, Rostami AB, Jafarkazemi F. Aerodynamic analysis of the boundary layer region of symmetric airfoils at ground proximity. Aerosp Sci Technol. 2012; 17: 7–20.
10. Papoutsis-Kiachagias EM, Papadimitriou DI, Giannakoglou KC. Discrete and continuous adjoint methods in aerodynamic robust design problems. In: Proceedings of an ECCOMAS Thematic Conference; Antalya, Turkey. 2011 May; 61–64.
11. Ma R, Liu P. Numerical simulation of low-Reynolds-number and high-lift airfoil S1223. In: Proceedings of the World Congress on Engineering, 2009 Jul 1–3; London, UK. 2009; II: 1–6.
12. Koch PN, Wujek B, Golovidov O, Simpson TW. Facilitating probabilistic multidisciplinary design optimization using Kriging approximation models. AIAA Paper 2002–5415; 2002 Sep.
13. Deb K. Multi-objective optimization using evolutionary algorithms. Chichester: John Wiley & Sons; 2001.
14. Fonseca CM, Fleming PJ. Genetic algorithms for multi-objective optimization: formulation, discussion and generalization. In: Proceedings of the 5th International Conference on Genetic Algorithms; San Mateo, CA, USA. 1993; 416–423.
15. Drela M, Giles MB. Viscous-inviscid analysis of transonic and low Reynolds number airfoils. AIAA J. 1987; 25(10): 1347–1355.

 